MONOCULAR DIPLOPIA DUE TO SPHEROCYLINDRICAL REFRACTIVE ERRORS (AN AMERICAN OPHTHALMOLOGICAL SOCIETY THESIS)

BY Steven M. Archer MD

ABSTRACT

Purpose: Ordinary spherocylindrical refractive errors have been recognized as a cause of monocular diplopia for over a century, yet explanation of this phenomenon using geometrical optics has remained problematic. This study tests the hypothesis that the diffraction theory treatment of refractive errors will provide a more satisfactory explanation of monocular diplopia.

Methods: Diffraction theory calculations were carried out for modulation transfer functions, point spread functions, and line spread functions under conditions of defocus, astigmatism, and mixed spherocylindrical refractive errors. Defocused photographs of inked and projected black lines were made to demonstrate the predicted consequences of the theoretical calculations.

Results: For certain amounts of defocus, line spread functions resulting from spherical defocus are predicted to have a bimodal intensity distribution that could provide the basis for diplopia with line targets. Multimodal intensity distributions are predicted in point spread functions and provide a basis for diplopia or polyopia of point targets under conditions of astigmatism. The predicted doubling effect is evident in defocused photographs of black lines, but the effect is not as robust as the subjective experience of monocular diplopia.

Conclusions: Monocular diplopia due to ordinary refractive errors can be predicted from diffraction theory. Higher-order aberrations—such as spherical aberration—are not necessary but may, under some circumstances, enhance the features of monocular diplopia. The physical basis for monocular diplopia is relatively subtle, and enhancement by neural processing is probably needed to account for the robustness of the percept.

Trans Am Ophthalmol Soc 2007;105:252-271

INTRODUCTION

Monocular diplopia or polyopia can be experienced by almost everyone under certain circumstances. Phenomena such as the doubling of the horns of a crescent moon, splitting of a fine white line on a black or a black line on a white background—all made more pronounced by defects of focus—have been repeatedly mentioned in the literature over many years.[1,2] Monocular diplopia accounted for 25% of diplopia cases presenting to an ophthalmic casualty department.[3] Yet when presented with a complaint of diplopia, clinicians often overlook monocular causes, presuming the problem to be of binocular origin.

Monocular diplopia due to nonoptical causes is extraordinarily rare. Psychiatric disease or malingering is often suspected[4,5]; however, Morris[3] found that most cases have an organic explanation. Monocular diplopia associated with neurologic lesions has been described.[6] Sensory adaptations to strabismus[7-10] and treatment of amblyopia[11] can produce monocular diplopia. A few cases of monocular diplopia with retinal pathology have been reported.[3,4]

The vast majority of monocular diplopia, however, is optical in origin.[12] Some optical etiologies are relatively easy to understand. Extrapupillary apertures such as with iridodialysis or iridectomy can function as a Scheiner's disc.[13,14] Lens abnormalities such as cataract, subluxation, or other lenticular abnormality[12,14,15] and corneal abnormalities such as keratoconus or other corneal pathology[5,16,17] can result in monocular diplopia. Monocular diplopia can result from pressure on the cornea by a chalazion[14,18] or by the eyelids during prolonged reading, near work, or television viewing.[19-24] Corneal aberrations after refractive corneal surgery are an increasingly important cause of monocular diplopia.[25-29] Reflections from spectacle lens surfaces[30,31] have been implicated in monocular diplopia. Although it is usually subclinical, being either unnoticed or regarded as a normal state of affairs by those who observe it, the most common monocular diplopia is that occurring in otherwise normal eyes, with or without refractive errors.

PHYSIOLOGICAL MONOCULAR DIPLOPIA

Fincham[32] stated that physiological monocular diplopia occurs in 40% to 50% of otherwise normal eyes. It can be cause for clinical complaint[33] but is usually so minor that only the occasional highly perceptive patient with otherwise good vision will remark about it spontaneously. Most individuals are unaware of it until it is demonstrated to them under special testing conditions. A bright line on a dark background is a particularly effective stimulus for eliciting physiological monocular diplopia,[8,32] which is characterized by a faint secondary image that is displaced 3 to 6 minutes of arc upward from the primary image. Moving a pinhole in front of the eye will cause a jump from one image to the other, and blocking the upper or lower portion of the pupil with a card will usually eliminate the second image.[8,32,33] Taken together, these findings suggest that variation of the refractive power from one area of the pupillary aperture to another is the cause of the diplopia.

Guyton[8] states that the cornea is responsible for 40% of the optical aberrations resulting in monocular diplopia, with the crystalline lens being responsible in roughly 60% of cases. Rubin[12] suggests that minor imperfections in the optical system of the eye, such as the optical axes of the cornea and lens not being coincident, are the cause. In a study of 70 individuals with normal visual acuity, Fincham[32] found that differences of 0.5 diopter or more in refractive power between the upper and lower portions of the pupil correlated with the observation of this form of physiological monocular diplopia. Uncorrected spherocylindrical refractive error is not

From the Department of Ophthalmology and Visual Sciences, University of Michigan, Ann Arbor.

necessary for physiological monocular diplopia, which occurs in spite of full optical correction; yet Fincham found that in some cases the diplopia was enhanced by simulation of myopia with the introduction of a weak positive lens. He also noted that astigmatism could produce a more distinct doubling of a bright line in some axes with a dark space appearing between the two images, which is different from the description of typical physiological monocular diplopia and may represent a different phenomenon altogether.

ORDINARY SPHEROCYLINDRICAL REFRACTIVE ERRORS

Monocular diplopia occurring with ordinary refractive errors has been recognized by clinicians since at least the 19th century, when Bull[34] concluded that "all eyes and in every case of refractive error, including the common cases of myopia and hypermetropia, the many varieties of astigmic vision, and the case of objects slightly outside the *p.r.* or the *p.p.*, there is to be found the phenomenon usually denoted by the term *monocular diplopia*…." Scott[35] states that monocular diplopia due to myopia or myopic astigmatism is the most common form of nonstrabismic diplopia that he sees. Uncorrected simple astigmatism was implicated as the cause in two cases from Stampfer and Tredici's series of flying personnel with monocular diplopia,[14] and simulated astigmatism reproducibly results in diplopia experimentally.[36]

Case Reports

The following cases have been selected to illustrate how, even when the referring ophthalmologist is aware of the potential for ordinary refractive errors to cause diplopia, the correct diagnosis can be missed, especially when there is a coexisting condition to which the diplopia could be attributed.

Case 1. A 7-year-old boy is referred for a complaint of diplopia. The uncorrected visual acuity is 20/20 in the right eye and 20/40 in the left eye. On further testing, the diplopia is monocular, worse in the left eye than the right, and relieved with a pinhole. Cycloplegic retinoscopy shows a refraction of –0.75 + 0.75 × 90 in the right eye and –1.00 + 0.50 × 90 in the left eye.

It is unusual for children to have perception so acute that they would complain about the diplopia with refractive errors. This case illustrates that sometimes relatively small refractive errors are particularly efficient at eliciting this complaint.

Case 2. A 63-year-old man is referred by his cornea surgeon for a complaint of diplopia in his pseudophakic eye 1 week after cataract surgery. His manifest refraction in the cornea surgeon's office was –1.50 + 2.50 × 110 that results in an acuity of 20/60. Retinoscopy shows a refraction of –3.50 + 6.00 × 110 that results in an acuity of 20/25. This refraction eliminates his diplopia, and he is referred back to his cornea surgeon for cutting of a suture.

The monocular diplopia in this case was due to a large amount of astigmatism. The astigmatism was not fully appreciated on manifest refraction because it was so far outside of the expected range.

Case 3. A 55-year-old dentist is referred for complaint of monocular diplopia, worse in the right eye than the left for 5 months. He has a history of amblyopia in the right eye and esotropia but has had no strabismus surgery. His visual acuity is 20/160 in his right eye and 20/20 in his left eye with his current spectacles, which measure –2.00 + 2.00 × 100 in the right eye and –1.50 + 0.25 × 70 in the left eye. His motility examination shows a 5Δ esotropia at near and a 6Δ esotropia and 2Δ right hypertropia at near.

A 5Δ base-out prism provides minimal improvement. A pinhole eliminates the diplopia in either eye. Retinoscopy shows a refraction of –4.75 + 1.00 × 75 in the right eye that improves the acuity to 20/60 and eliminates the diplopia. Manifest refraction of the left eye is –1.75 +0.50 × 70 and eliminates the "shadowing" in that eye.

The diplopia in this case is due to undercorrection of myopia in the amblyopic right eye. In spite of the temptation to attribute his problems to the strabismus and amblyopia history, this patient comes with a description of diplopia that is clearly monocular. The reason that this case was not diagnosed by the referring ophthalmologist stems from the difficulty in obtaining an accurate subjective refraction in an amblyopic eye, along with the failure to recognize that, as is the case with strabismic diplopia, an eye with reduced vision is still sometimes capable of producing a complaint of diplopia.

Case 4. A 90-year-old bilaterally pseudophakic woman with a 6-year history of diplopia, satisfactorily corrected with prism in her spectacles until 6 months previously, is referred because her ophthalmologist was now unable to find any prism that eliminates her diplopia. Her vision is 20/30- in each eye with her current spectacles, which measure –0.25 + 1.00 × 38 in the right eye and –1.25 + 3.25 × 175 in the left eye with 1.5Δ base-out in each eye. Her motility examination shows 6Δ of esotropia in primary position at distance that increases to 14Δ in right gaze. At near she is orthophoric.

Her esotropia in primary position is neutralized by a total of 6Δ base-out prism, but she continues to complain of seeing multiple strokes on each letter on the eye chart. On further investigation, it is found that this is not eliminated by covering either eye and is eliminated with a pinhole. Retinoscopy shows a refraction of –2.75 + 2.25 × 25 in her right eye and –2.75 + 1.25 × 10 in her left eye. This does not improve her acuity but eliminates the multiple strokes on the letters and, along with 6Δ base-out prism, eliminates all of her diplopia.

This patient has strabismus due to a slowly progressive sixth nerve palsy (and was subsequently referred to a neuro-ophthalmologist for evaluation). When prismatic correction of the esotropia did not eliminate her diplopia, the remaining diplopia needed to be re-investigated to discover that she also has bilateral monocular diplopia due to inadequate correction of her refractive error.

Case 5. A 60-year-old woman is referred for diplopia that she has had ever since 2 pars plana vitrectomies and membrane peeling in her right eye 2 years ago. She reports that the diplopia is worst when reading, there is a size difference in the images of the 2 eyes and that the image in the right eye is distorted. She has a history of "lazy eye" as a child and is pseudophakic in her right eye. Her visual acuity is 20/30 in the right eye and 20/20 in the left eye with her current spectacles, which are plano + 1.00 × 135 in the right

eye and +0.75 + 0.50 × 90 in the left eye. Her motility examination shows a 12Δ intermittent exotropia at near and a 5Δ intermittent exotropia at distance.

A pinhole over the right eye eliminates the diplopia. Retinoscopy shows a refraction of +0.25 + 0.50 × 10. This refraction, along with 1Δ base-up in the right eye (along with the same +2.50 addition for reading that she had in her present spectacles) produced a dramatic subjective improvement in her reading vision and eliminated her diplopia.

This patient's diplopia could have been attributed to her convergence insufficiency pattern intermittent exotropia, or metamorphopsia of retinal origin. Further investigation revealed that most of her symptoms were due to the small amount of astigmatic correction in her right spectacle lens that was 55º from the correct axis.

Demonstration

Most people can experience the diplopia that accompanies optical defocus for themselves. Scott[35] offers a demonstration of diplopia with myopic defocus. He instructs the reader to hold a black thread in front of a bright background at a distance of 2 feet and to focus monocularly on a finger held between the eye and the thread. As the finger is brought closer to the eye (that is, the image of the thread falls further in front of the retina), the thread will blur and then become distinctly double, with the images of the thread becoming increasingly separated as the finger is brought closer to the eye. In this demonstration, Scott does not note diplopia when focusing on a finger held further from the eye than the thread. However, a fine black line on white paper, viewed monocularly, can be used to demonstrate diplopia with hyperopic defocus in most individuals.[14] As the paper is moved closer to the eye than the near point of accommodation (the image of the line falls behind the retina), doubling, trebling, or even quadrupling of the line can be observed. This phenomenon can be utilized as the end point in testing for the near point of accommodation with the "accommodation test" on the back of a widely distributed version of the Lebensohn near card. As the card is brought closer to the eye, the 2 fine parallel black lines appear to be 3 lines when the innermost of the second images of each line overlap, indicating that a degree of hyperopic defocus has occurred.

Coffeen and Guyton[37] showed experimentally that most people are able to appreciate monocular diplopia with both hyperopic and myopic defocus. By inducing myopic refractive errors in otherwise normal test subjects, they found that 9 of 11 eyes experienced doubling of black lines on a white background, either projected on a screen or inked on white paper. With induced hyperopia, 7 of 11 eyes experienced diplopia with projected lines and 9 of 11 with inked lines. On average, diplopia developed with –1.57 D of myopic defocus when projected lines were used and –2.19 D with inked lines. The average amount of hyperopic defocus needed to produce diplopia was +1.14 D and +1.69 D for projected and inked lines, respectively.

On the other hand, Guyton[8] at one time stated that simple refractive errors such as myopia, hyperopia, and astigmatism do not cause diplopia. This statement—despite reports to the contrary and the daily personal experience of those of us with uncorrected mild myopia—is perhaps a reflection of the difficulty in imagining a plausible mechanism by which ordinary spherocylindrical refractive errors could cause diplopia.

Geometrical Optics

Attempts to explain the doubling of an image in a defocused human eye have relied almost exclusively on geometrical optics analysis. In geometrical optics, the defocused image of a point (point spread function) is a blur circle of uniform intensity. The diameter of the blur circle increases as the image falls further in front of or behind the retina, but the form of the point spread function is always a circle. The image of a line (line spread function) under conditions of defocus can be obtained by imagining a series of defocused points falling along the line. Integrating along vertical chords through the blur circle of the point spread function (Figure 1) gives the intensity of the line spread function at a given eccentricity from the center of the line (Figure 2).[38,39] Like the point spread function, the scale of this line spread function changes with increasing defocus, but its form does not. It is clear that doubling of a fine white line on a dark background cannot be explained by the geometrical optics of simple defocus alone.

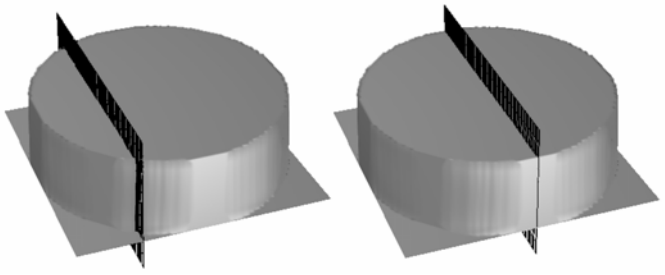

FIGURE 1

The line spread function is calculated by integration along chords through the point spread function.

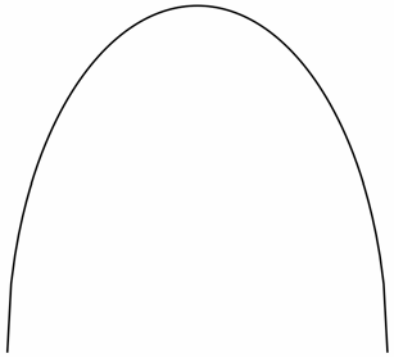

FIGURE 2

The intensity profile of a defocused line (line spread function) according to the principles of geometrical optics.

Analysis of the blurred image of a black line on a white background is more involved. A black line can be regarded as a gap between 2 bright edges. An edge can be constructed as the summation of a series of parallel lines, the intensity at positions near the edge being the sum of the contributions from all of the lines on the bright side of the edge close enough that their line spread functions overlap that position. The edge spread function can therefore be computed as the running integral of the line spread function (Figure 3).[38,39] Two of these edges can then be superimposed with various amounts of separation to model black lines of various widths (Figure 4). With the defocused edge spread function predicted from geometrical optics, there is no separation of the edges that produces a band of increased intensity in the dark gap between the 2 edges that could give rise to monocular diplopia (Figure 5).

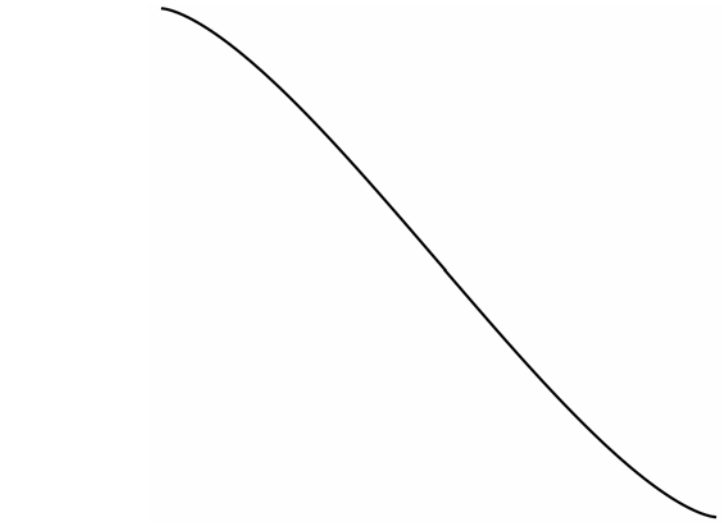

FIGURE 3

The intensity profile of a defocused edge between white and black areas (edge spread function) according to the principles of geometrical optics.

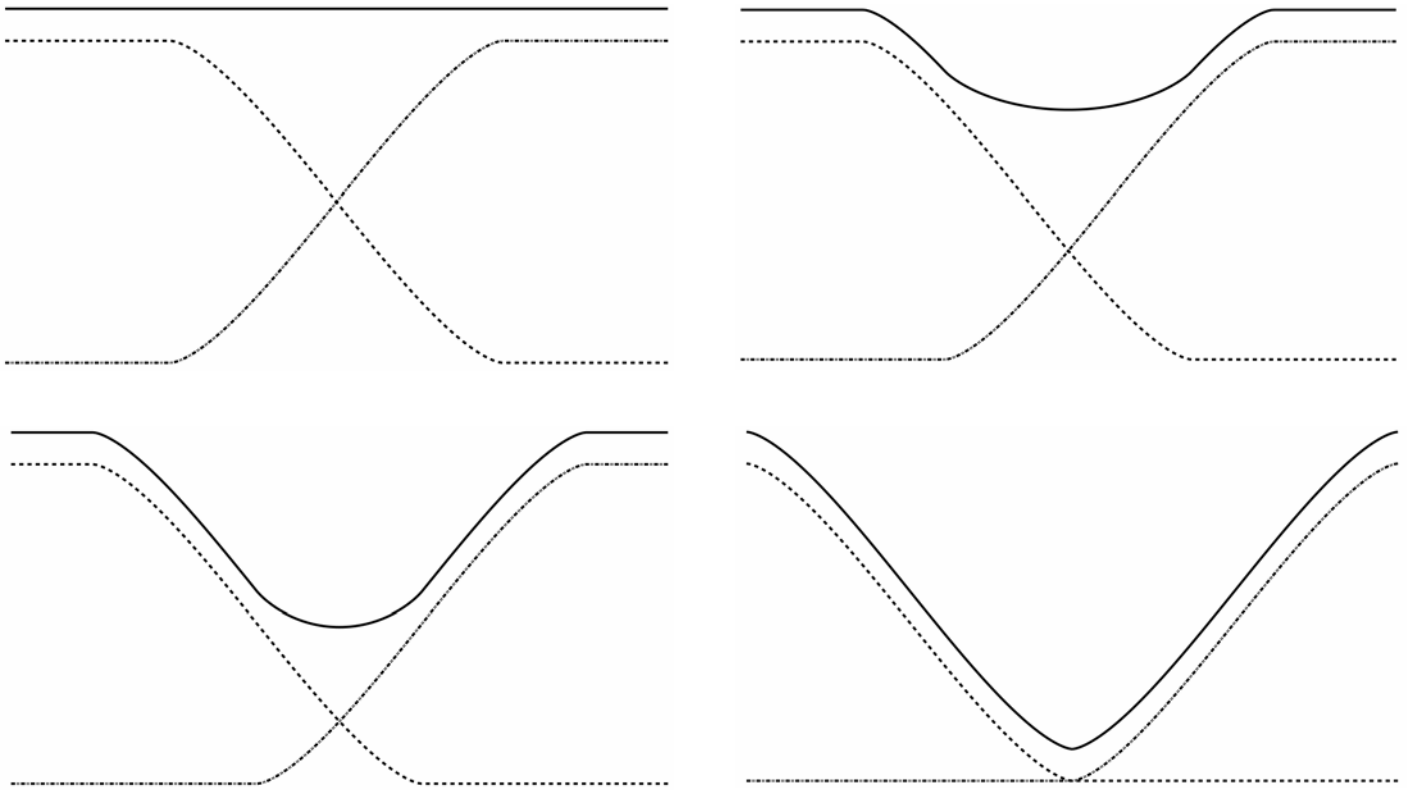

FIGURE 4

A defocused black line is constructed from 2 defocused edges (dashed lines). The summation of the 2 edges (solid line) has been shifted upward for clearer visualization. A,Top left, When the edges abut, the result is a field of uniform intensity. Top right and Bottom, As the edges are separated, a deepening depression in the intensity profile develops between them.

Coffeen and Guyton[37] conclude that an inflection in the defocused edge spread function, an exaggerated but unrealizable example of which is shown in Figure 6, is needed in order to produce doubling of a black line on a white background (Figure 7). Figure 8 shows that, with the hypothetical defocused edge spread function shown in Figure 6, a bright band develops in the gap when the separation is less than approximately 50% of the width of the line spread function. Differentiation of the edge spread function returns the form of the line spread function from which it was formed (Figure 9). It is obvious that with this line spread function, monocular diplopia of a fine white line on a dark background can be accounted for as well.

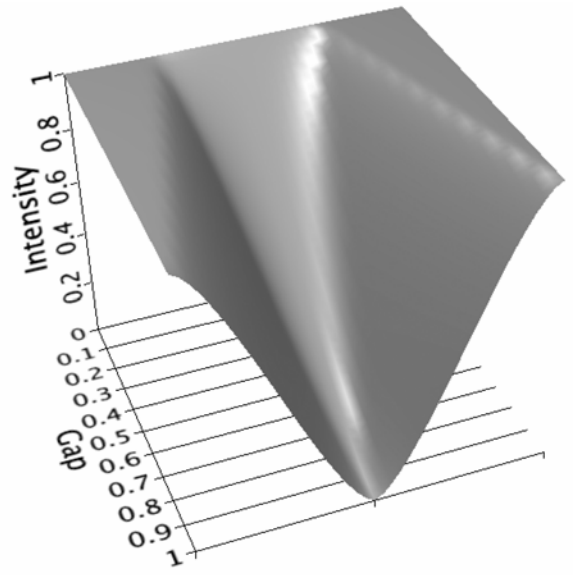

FIGURE 5

The intensity profile of a defocused black line as a function of the gap between the 2 edges of which it is composed. The gap distance is plotted as a fraction of the edge spread width. With the defocused edge spread function derived from geometrical optics, there is no gap distance at which there is an intensity ridge in the gap between the 2 edges that could give rise to the perception of doubling of the black line.

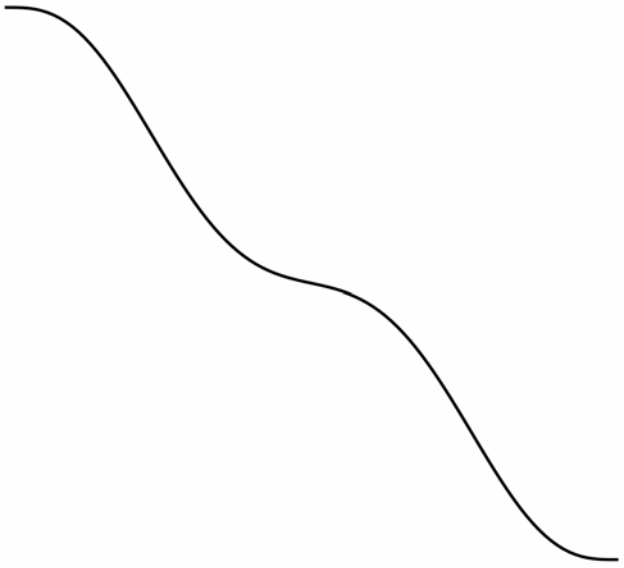

FIGURE 6

A hypothetical defocused edge spread function with the inflection that is necessary to produce monocular diplopia.

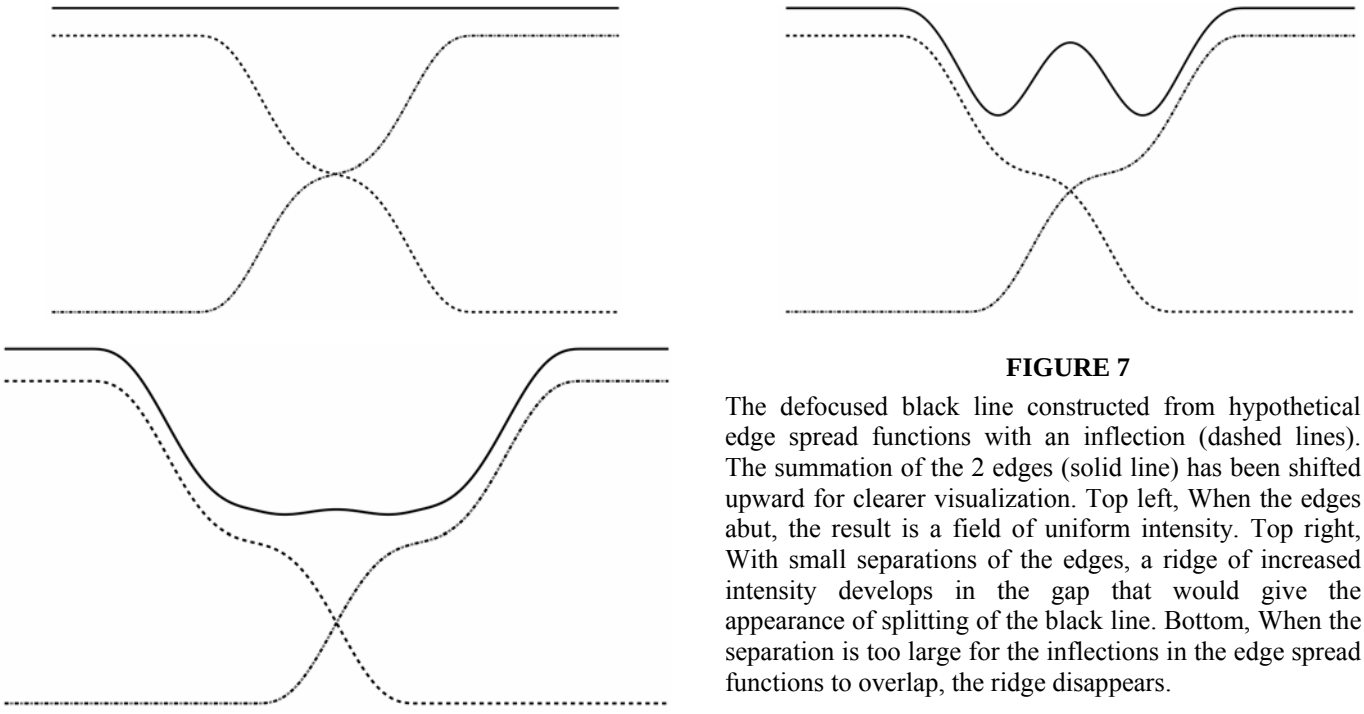

FIGURE 7

The defocused black line constructed from hypothetical edge spread functions with an inflection (dashed lines). The summation of the 2 edges (solid line) has been shifted upward for clearer visualization. Top left, When the edges abut, the result is a field of uniform intensity. Top right, With small separations of the edges, a ridge of increased intensity develops in the gap that would give the appearance of splitting of the black line. Bottom, When the separation is too large for the inflections in the edge spread functions to overlap, the ridge disappears.

Thus, a bimodal line spread function implied by the doubling of a fine white line on a black background also appears to be a sufficient condition for doubling of a fine black line on a white background. But how could a bimodal line spread function be produced by simple defocus? Because geometrical optics offers no possible mechanism by which this might occur, many investigators have postulated that additional aberrations—usually spherical aberration—must be present to account for the observed phenomena.[30,35,37,40,41] Ray-tracing analysis suggests that negative spherical aberration in myopic eyes[30,35] and positive spherical aberration in hyperopic eyes[30,41] could produce the bimodal line spread needed to explain monocular diplopia. However, explanation of monocular diplopia with both positive and negative defocus in the same eye, as found by Coffeen and Guyton, requires a complicated pattern of aberration[37,40] that seems unlikely to occur as consistently as the phenomenon of monocular diplopia.

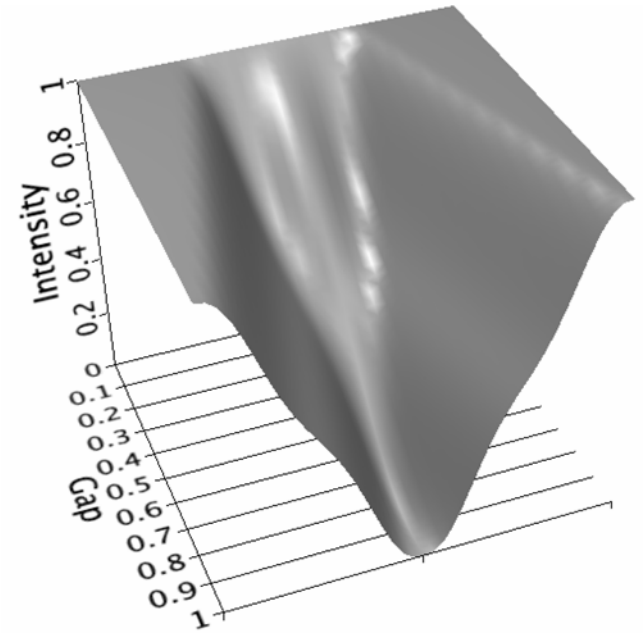

FIGURE 8

The intensity profile of a defocused black line as a function of the gap between two hypothetical edge spread functions with an inflection. An intensity ridge giving the perception of splitting of the black line develops in the gap when the separation between the edges is less than half the width of the edge spread function.

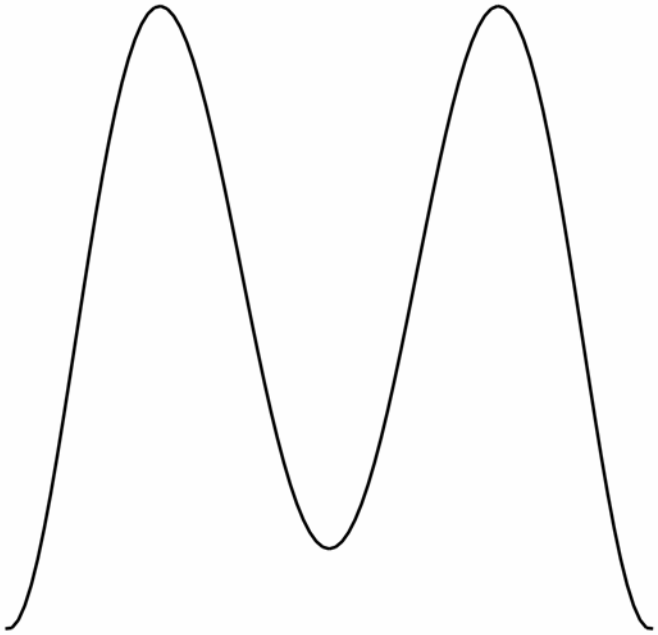

FIGURE 9

The bimodal intensity profile of the line spread function that gives rise to the theoretical edge spread function shown in Figure 6, which is capable of producing monocular diplopia with a black line target.

Diffraction Theory

Geometrical optics is a special case of diffraction theory in which the limit of the wavelength of light approaches zero.[42] This simplification yields a useful approximation of the properties of an optical system—such as the human eye—in many respects[38,43-45]; however, the results can differ from diffraction theory in the fine structure of image formation, especially for small amounts of defocus. In undertaking analysis by diffraction theory, it is often convenient to evaluate the performance an optical system in terms of its spatial frequency response (modulation transfer function). The modulation transfer function of a defocused eye can be calculated theoretically.[38,46] Point spread and line spread functions can be computed from the modulation transfer function by inverse Fourier transformation[39,47]; however, this methodology has not, to my knowledge, been applied to theoretical modulation transfer functions of a defocused eye in the context of accounting for the monocular diplopia that arises from ordinary refractive errors.

Hypothesis

When image formation in an eye is modeled using diffraction theory, point spread and line spread functions under conditions of defocus and astigmatism—without invoking higher-order aberrations—will be found to have inherent characteristics that provide a basis for monocular diplopia.

METHODS

THEORETICAL CALCULATIONS

Computations assumed a 3-mm-diameter entrance pupil and light with a wavelength of 555 nm, although results can be scaled for other wavelengths or pupil diameters. After Hopkins,[43] the amount of defocus is characterized by $w_{20}=n\lambda/\pi$, where w_{20} is the distance between the defocused and aberration-free wavefront at the edge of the pupil and λ is the wavelength. An n of 20 is equivalent to approximately 3 D of defocus in an eye with a 3-mm entrance pupil and a reduced focal length of 16.78 mm. Calculations were made for increasing amounts of defocus, n, in increments of 1.

Diffraction in an optical system with a finite pupil acts as a low-pass spatial frequency filter with an absolute spatial frequency cutoff,[46,48,49] making it possible to satisfy the conditions of the sampling theorem[50,51]; thus, image formation in the eye is suitable for analysis using discrete Fourier transform techniques. Algorithms for the computation of Bessel functions[51] and discrete inverse fast Fourier transforms[50,51] were custom-programmed in JSL, executed and results plotted using JMP versions 5.1.1 through 6.03 (SAS Institute Incorporated, Cary, North Carolina).

Modulation Transfer Function

Several approaches to the computation of modulation transfer functions for defocused Fraunhofer diffraction images have been described.[43,52] In this study, the method described by Hopkins[43]—which expresses the modulation transfer function as a computationally efficient convergent series of Bessel functions—was used. The frequency response was calculated at 0.46 cycle/degree intervals. Two-dimensional modulation transfer functions for astigmatic errors were calculated according to the computationally similar method described by De[53] at 0.88 cycle/degree intervals.

Line Spread Function

The line spread function and the modulation transfer function are related to each other by the Fourier transform.[48,54] In this study, the line spread functions for defocus were calculated by inverse discrete fast Fourier transform of the modulation transfer functions. Intensities were calculated at intervals of 4 seconds of arc.

Point Spread Function

In the radially symmetric case of simple defocus, the inverse Fourier transforms of the modulation transfer functions were computed by numerical integration of the inverse Hankel transform to obtain the point spread functions.[47,49] Intensities were calculated at intervals of 1 second of arc. Inverse 2-dimensional discrete fast Fourier transforms of the astigmatic modulation transfer functions were used to obtain point spread functions for astigmatic errors. Intensities were calculated at intervals of 4 seconds of arc.

PHOTOGRAPHIC DEMONSTRATIONS

The theoretical point spread and line spread functions should be directly applicable to the question of monocular diplopia occurring with defocused targets consisting of thin bright lines or bright points. However, the relationship of these results to monocular diplopia with commonly encountered real-world targets is more complex. To demonstrate the effects of defocus with black lines of finite width, inked lines on white paper created by a laser printer were photographed with a Nikon D100 camera with a Nikkor 24-85 mm lens used at an 85-mm focal length, *f*/8 (Nikon, Tokyo, Japan). The lines subtended approximately 0.45, 0.9, and 1.8 minutes of arc at the camera, respectively. The camera lens was adjusted for optimal focus, and a series of photos were then taken with the lens progressively defocused.

To obtain higher contrast, projected lines were used in the second photographic demonstration. A slide with black lines on a clear background was projected with an Ektographic III AM projector (Kodak, Rochester, New York) using a Vario-Prolux MC 70-120 mm *f*/2.8 lens (Schneider Optics, Hauppauge, New York) at a 120-mm focal length. The images were projected on screen (Da-Lite, Warsaw, Indiana) 3.2 m from the projector and photographed with the same Nikon camera from a distance of 3.6 m. The projector lens was focused optimally, and photographs of the screen were taken as the projector lens was progressively defocused.

RESULTS

THEORETICAL CALCULATIONS

Modulation Transfer Function With Defocus

The modulation transfer functions for selected amounts of defocus are shown in Figure 10. As expected, higher spatial frequencies initially suffer more reduction of contrast with defocus than lower spatial frequencies. However, at a certain level of defocus (Figure 10, top middle), the modulation transfer function begins to develop zero crossings with intervening bands of spatial frequencies that have negative contrast (Figure 10, top right, and bottom left, middle, and right). Negative contrast represents phase reversal and leads to the phenomenon of spurious resolution.[45,55] With increasing defocus, these zero crossings become more numerous and the bands of negative contrast migrate toward the lower spatial frequencies.

Point Spread Function With Defocus

Point spread functions for selected amounts of defocus, shown in Figure 11, show a shift of energy from the central peak out into the surrounding ring structure with defocus. As defocus increases, the point spread function cycles between maxima and minima at the

center. While having a minimum in the center of the point spread function is conducive to the formation of the bimodal line spread function needed to explain monocular diplopia, the diameter of the outermost ring structure will determine the spatial scale of the bimodal or multimodal line spread function.

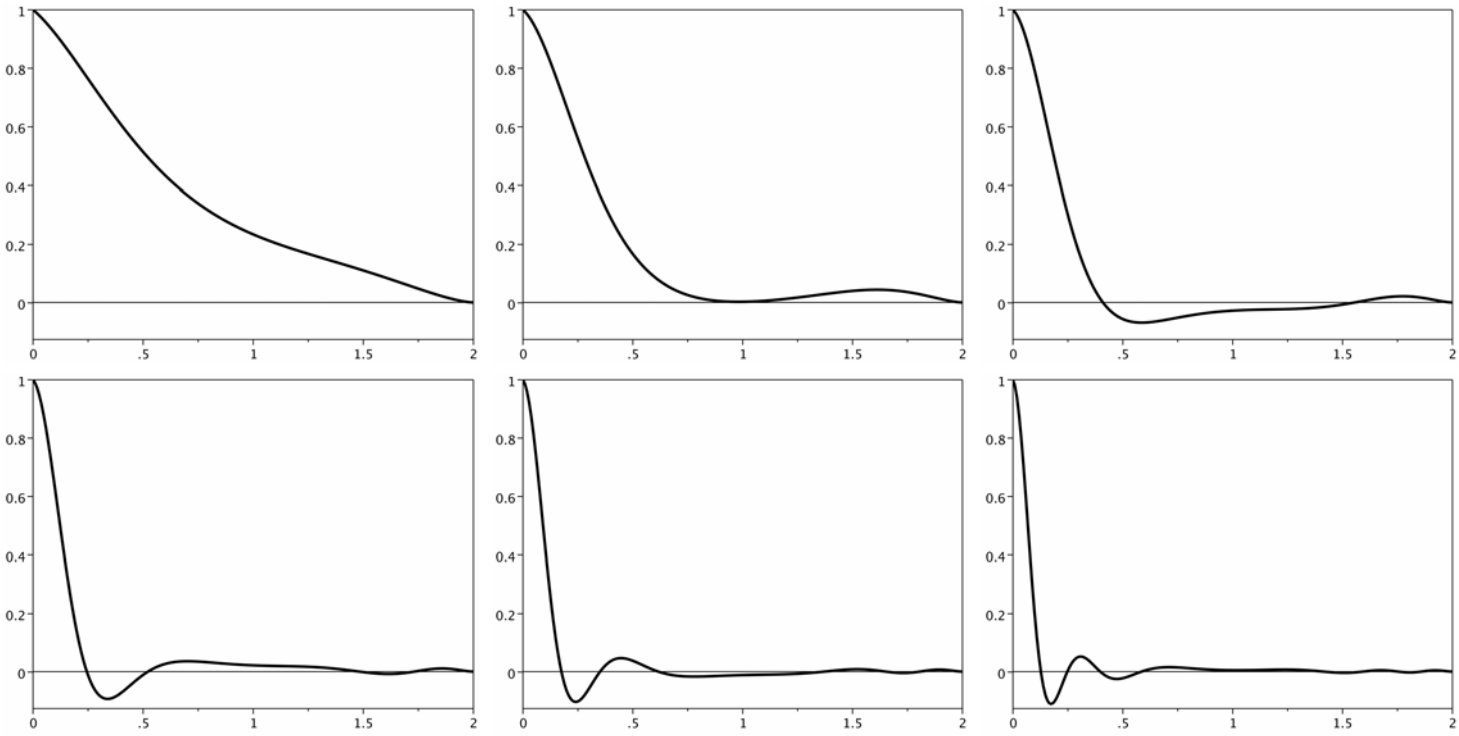

FIGURE 10

Modulation transfer functions calculated from diffraction theory for various amounts of spherical defocus, n. The vertical axis is the fraction of transmission. The horizontal axis is the spatial frequency, scaled according to the cutoff frequency for the aperture, which is normalized to a value of 2. In addition to reduced transmission that affects higher spatial frequencies more severely than lower spatial frequencies, phase reversals (negative regions of the modulation transfer function) develop with increasing defocus. Top left, n=1. Top middle, n=2. Top right, n=3. Bottom left, n=4.5. Bottom middle, n=6. Bottom right, n=8.

Line Spread Function With Defocus

Figure 12 shows the line spread functions for selected amounts of defocus. Certain amounts of defocus result in a bimodal intensity distribution on a spatial scale that should be readily perceived by a human eye and provides an obvious basis for monocular diplopia (Figure 12, top right). With further defocus, the increasingly complex line spread functions (Figure 12, bottom) recall the classic descriptions by von Helmholtz,[2] Bull,[34] Verhoeff,[40] and Emsley[1] of intricate banding as target lines are blurred beyond the initial perception of doubling.

Point Spread Function With Astigmatism

Pure astigmatic defocus—such as myopic astigmatism, in which the effects of the astigmatic error cannot be mitigated by accommodation—results in the point spread functions shown in Figure 13. In Figure 13, top right, it can be appreciated how astigmatism could produce a bimodal image and consequent monocular diplopia. Further defocus results in a multimodal intensity distribution and potential diplopia or polyopia (Figure 13, bottom). Note that while spherical defocus can result in diplopia with a line target, astigmatism can produce diplopia with even a point. From this observation, it might be expected that myopic astigmatism will be the most clinically important cause of monocular diplopia.

Point Spread Function With Astigmatism—Circle of Least Confusion

Figure 14 shows point spread functions for various amounts of astigmatic defocus in the plane of the circle of least confusion. This situation might occur with hyperopic astigmatism, where the patient is able to accommodate to place the circle of least confusion at the plane of the retina. Here, too, a multimodal point spread function potentially leads to polyopia from a single point, although it requires more defocus to produce these effects than with the previous forms of aberration.

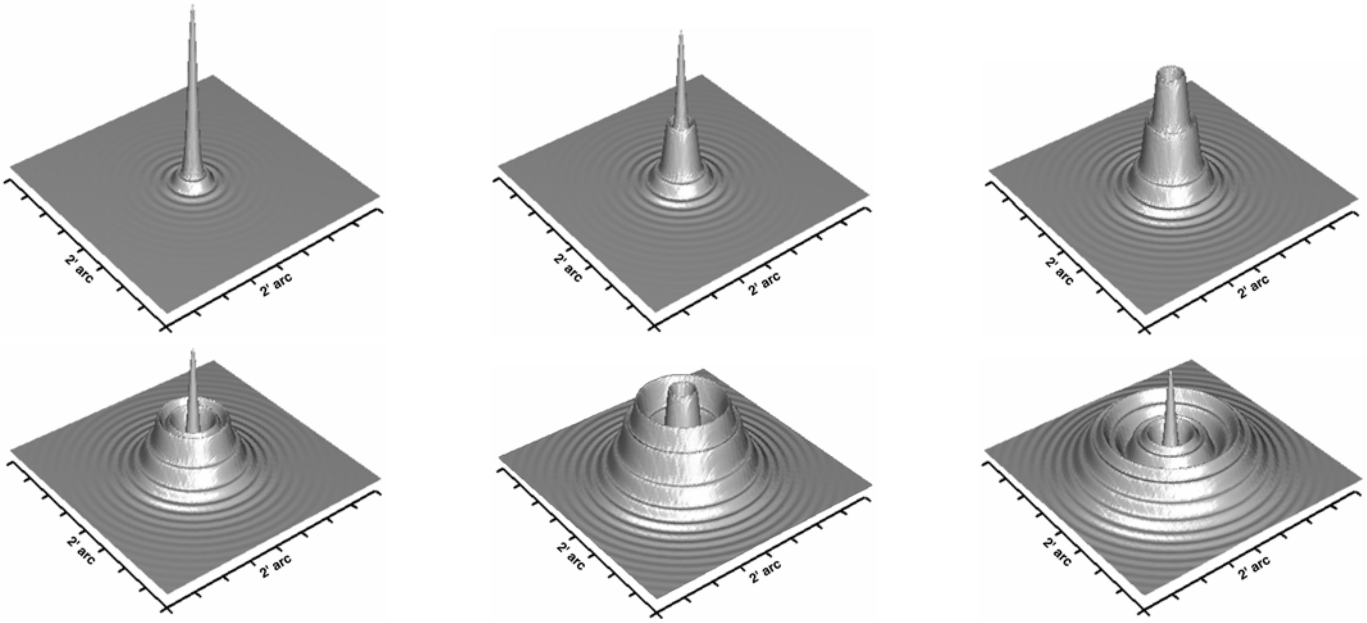

FIGURE 11

Point spread functions calculated from diffraction theory for various amounts of spherical defocus, n. The vertical axis, intensity, is linear but scaled proportionally to the log of the maximal value in each point spread function. With increasing defocus, the center of the point spread function cycles between maxima and minima. Top left, n=1. Top middle, n=2. Top right, n=3. Bottom left, n=4.5. Bottom middle, n=6. Bottom right, n=8.

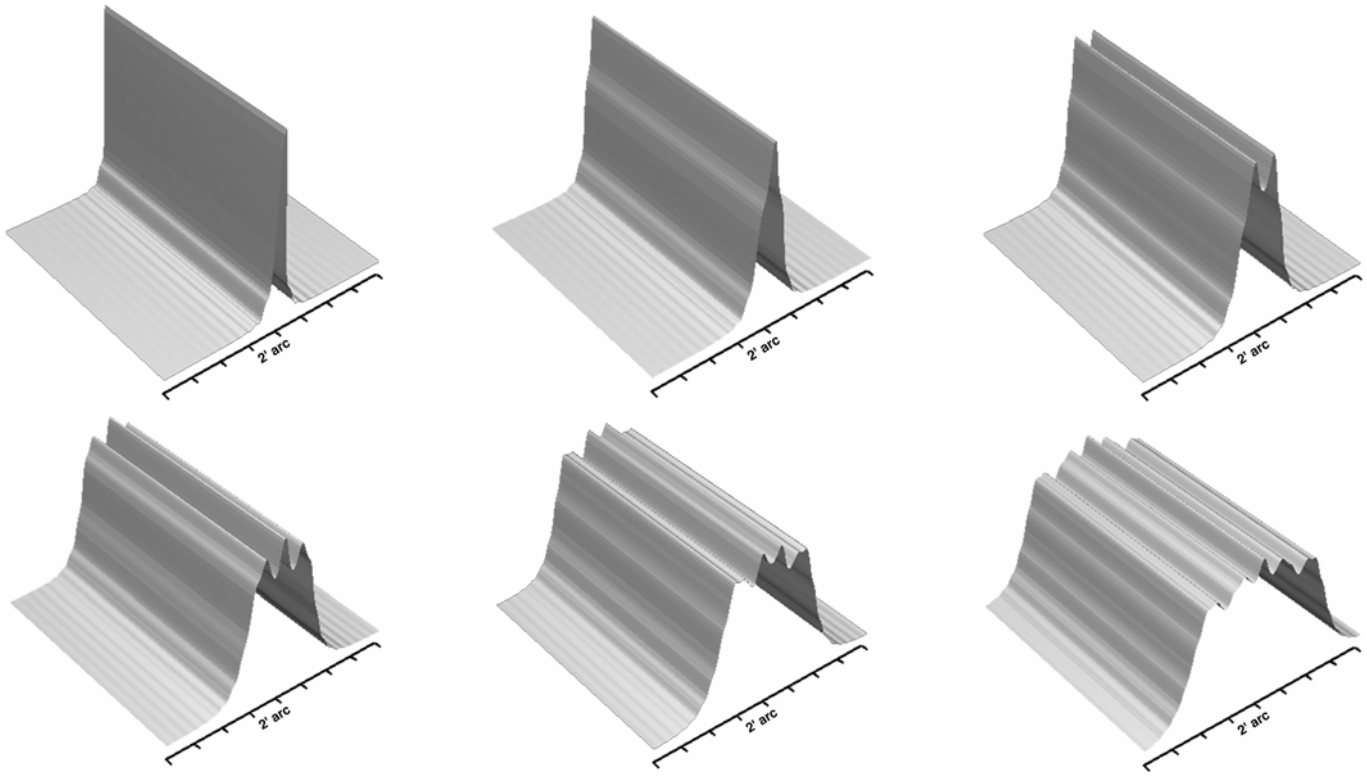

FIGURE 12

Line spread functions calculated from diffraction theory for various amounts of defocus, n. A bimodal line spread function develops for some amounts of defocus, forming the basis for monocular diplopia with spherical defocus of a bright line. Scaling is as in Figure 11. Top left, n=1. Top middle, n=2. Top right, n=3. Bottom left, n=4.5. Bottom middle, n=6. Bottom right, n=8.

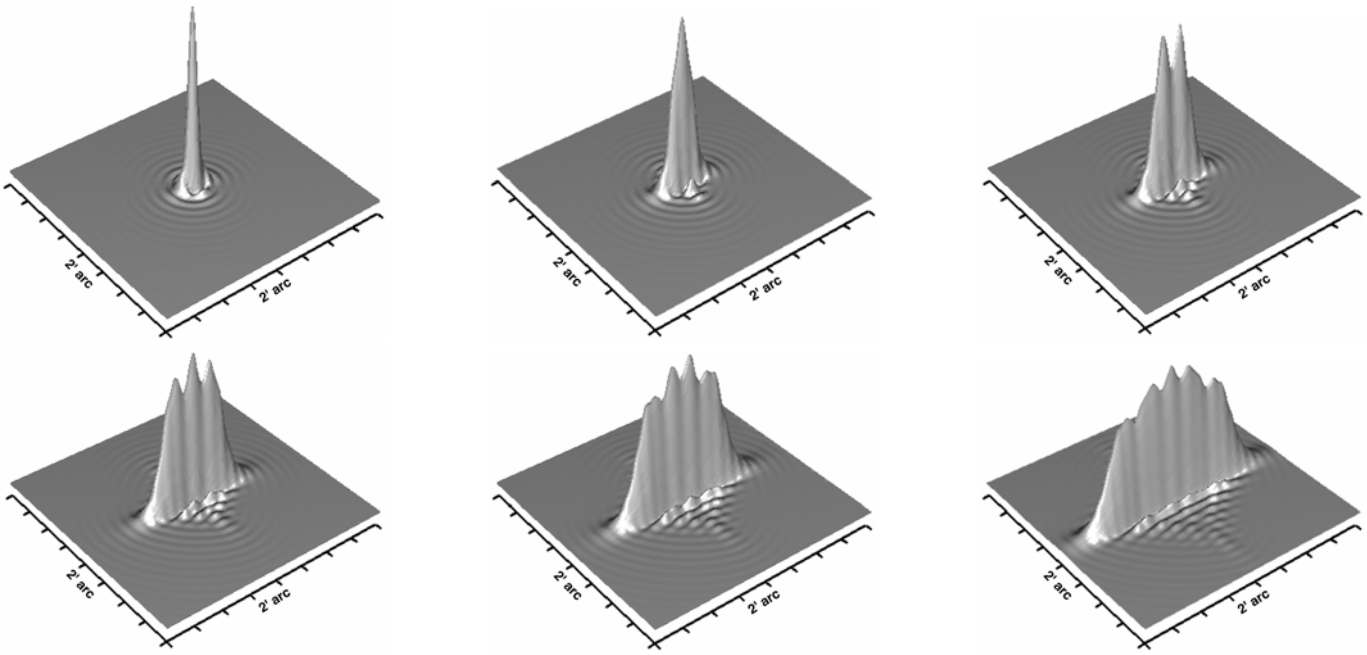

FIGURE 13

Point spread functions calculated from diffraction theory for various amounts of astigmatic error, n. A bimodal point spread function develops for some amounts of astigmatic error, forming the basis for monocular diplopia and polyopia of a bright point target. Scaling is as in Figure 11. Top left, n=1. Top middle, n=2. Top right, n=3. Bottom left, n=4.5. Bottom middle, n=6. Bottom right, n=8.

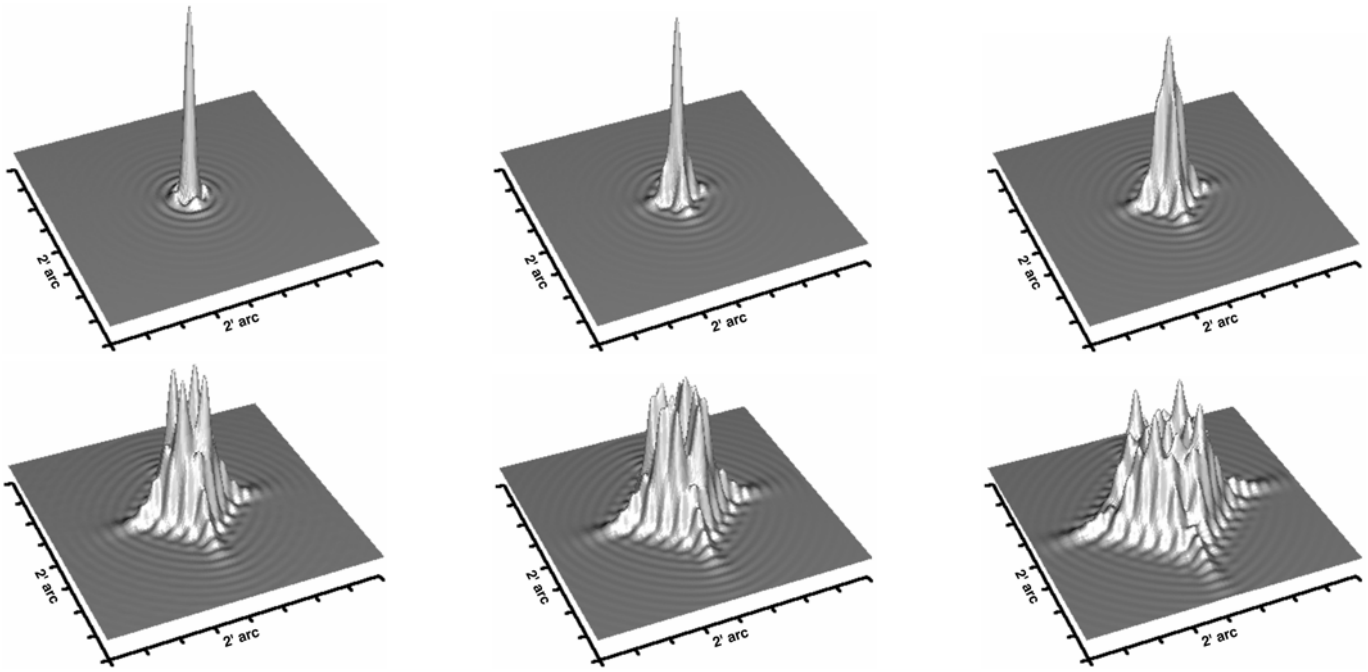

FIGURE 14

Point spread functions calculated from diffraction theory for various amounts of astigmatic error, n, combined with spherical defocus of –n/2 (in the plane of the circle of least confusion). This produces complex point spread functions that may give rise to polyopia with a bright point target. Scaling is as in Figure 11. Top left, n=1. Top middle, n=2. Top right, n=3. Bottom left, n=5. Bottom middle, n=6. Bottom right, n=8.

PHOTOGRAPHIC DEMONSTRATIONS

The defocused photographs taken directly of black lines on white paper are shown in Figure 15. Photographs of defocused projected lines are shown in Figure 16. In both tests, subtle light bands can be seen in the center of the blurred image of the black line. For wider lines, it takes progressively more defocus to produce the light bands. With large amounts of defocus, a very faint banding with multiple alternations between lighter and darker bands can be appreciated.

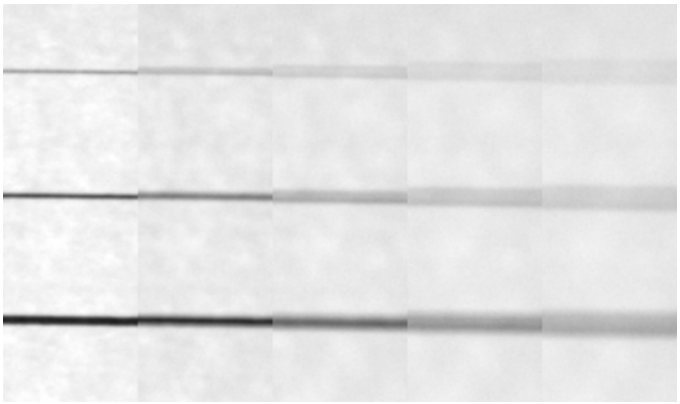

FIGURE 15

Monocular diplopia with spherical defocus of inked black lines. Black lines of different widths photographed with the camera lens increasingly defocused, from left to right (exposure compensation adjusted digitally).

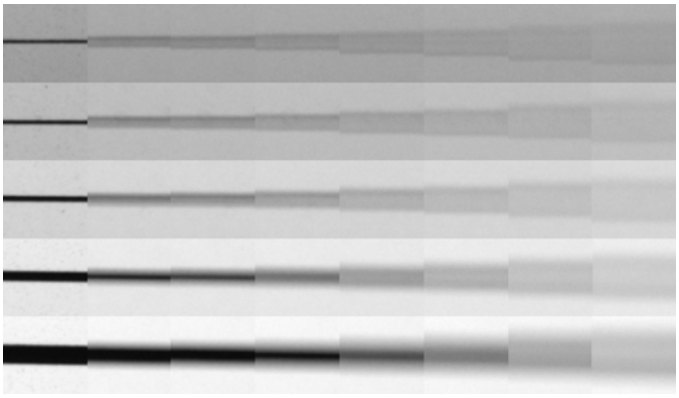

FIGURE 16

Monocular diplopia with spherical defocus of projected black lines. Black lines of different widths projected on a screen with the projector lens increasingly defocused, from left to right (exposure compensation adjusted digitally).

The photographic simulation of monocular diplopia occurring with defocus shown in Figures 15 and 16 is not as robust as that which is experienced in life. If anything, one might expect that a photographic lens, being closer to the ideal conditions of the theoretical calculations, would be better able to reproduce the line spread functions in Figure 12 than the optics of an eye. The difficulty of photographic demonstration is, indeed, part of what led previous investigators to conclude that it is not the defocus alone that is responsible for the diplopia.[34,40] There are a number of possible reasons why conventional photography may not be ideal for demonstrating monocular diplopia.

Many investigators believe that higher-order aberrations are important in the genesis of monocular diplopia.[30,35,37,40,41] A camera lens or, perhaps to a lesser extent, projector lens should suffer minimally from coma or irregular aberrations. Essentially identical images were obtained with comparable amounts of positive and negative defocus in these photographic demonstrations, indicating that these lenses are also well corrected for spherical aberration.[56] So, to whatever extent higher-order aberrations in a human eye contribute to monocular diplopia, photographic lenses will be less able to demonstrate the phenomenon. However, that monocular diplopia can be demonstrated with photographic lenses at all suggests that higher-order aberrations are not essential in its genesis.

These photographs were taken under conditions of white light. While this was done in order to match real world conditions under which monocular diplopia is observed, it does not match the monochromatic assumption used in the theoretical calculation of point spread and line spread functions. Longitudinal chromatic aberration was found by Campbell and coworkers[57] and by van Meeteren[58] to be the most important aberration affecting the modulation transfer function and producing retinal blur. Woods and coworkers[59] found that the contrast sensitivity function notches that they believe are related to monocular diplopia were easier to demonstrate with monochromatic than polychromatic light. Thus it may be that the relatively subtle bimodal feature of the line spread function with monochromatic light may be obscured by degradation of the fine details of the line spread function under polychromatic conditions. On the other hand, Krauskopf, [60] using a double-pass method, found the in-focus modulation transfer function to be no better with monochromatic light than with white light, and the results with white light compare favorably to monochromatic results in other related experiments as well.[38,61,62]

Another difficulty arises from the longer focal length of the camera lens than the eye. For example, at $f/4$, an 85-mm lens has an aperture of a little over 21 mm. Because the spatial scale is in inverse proportion to the pupil diameter, the initial split of the peaks in the line spread function with defocus will be separated by only about 17 seconds of arc. Demonstrating this will pose difficult requirements for camera resolution. Even with sufficient resolution, the thinness of the target line will make it difficult to provide sufficient light for imaging. Thus, more defocus was needed to create higher-order ring structures that are large enough to easily image; however, these higher-order rings do not produce troughs in the line spread function with as much contrast as the initial defocus ring. The scale of the diffraction image can be enlarged by going to a smaller aperture or higher f stop, lessening the resolution requirements of the camera, but this makes the light availability problem worse and the increased depth of field makes it difficult to obtain a sufficient range of defocus. Obtaining adequate image intensity is much easier to accomplish, and indeed

diffraction effects are easy to demonstrate, with laser illumination; however, diffraction with coherent light is not comparable and gives different results than illumination with incoherent light.

As will be discussed below, there are constraints on the trough in the middle of the line spread function and the peak in the blurred image of a black line that limit them to very low contrast. The image captured photographically may actually be representative of the retinal image; however, the edge contrast enhancement that occurs in the retina[44] may result in a stronger percept of line splitting than the physical image would suggest. In support of this explanation is the fact that the line doubling is much more distinct in the viewfinder as the picture is being taken than in the image captured by the camera. This may be because the image that the eye obtains through the viewfinder is on a scale similar to that over which edge contrast enhancement normally operates, whereas the photograph is displayed on a larger scale. The more pronounced doubling seen in the viewfinder cannot be due to aberrations in the eye because viewing the viewfinder through a pinhole does not reduce the effect; if anything, it becomes more distinct through a pinhole.

DISCUSSION

That diffraction, with or without various aberrations, produces point spreads with complicated features is well known. The predicted point spreads can be demonstrated experimentally on the optical bench.[56] However, the implications with respect to monocular diplopia have not been widely appreciated, perhaps because studies based on a diffraction model are often more concerned with characterizing image formation in the spatial frequency domain (modulation transfer function) rather than the structure of the image itself.

Point spread functions similar to those in Figure 11 were obtained by Wilson and coworkers[63] using aberrometry data from individual eyes and computationally simulating defocused point spread functions for 1-mm pupils (except defocus, essentially the aberration-free diffraction limited case). With 5-mm pupils, more complicated patterns arose because of the inclusion of higher-order aberrations in the calculation, but the point spread functions still preserve the ring structure, although it is asymmetric for myopic and hyperopic defocus. Artal,[64] using a similar technique (measured aberrations included in the computation of defocus) to simulate defocus, also found maxima and minima in the resulting point spread function leading to doubling of features in the formation of an image.

COMPARISON WITH EXPERIMENTALLY MEASURED DEFOCUSED RETINAL IMAGES

Losada and Navarro[65] imaged the point spread in human eyes with small amounts of defocus and astigmatism by a double-pass method, but the pattern was complicated and it is difficult to say how it pertains to monocular diplopia. A basis for monocular diplopia was also not obvious in the images of the point spread of defocused eyes obtained by Villegas and colleagues.[66]

Direct measurement of the line spread in defocused human eyes with a double-pass method has also not confirmed the bimodal shape needed to explain monocular diplopia.[38,67] However, failure to find a basis for monocular diplopia in measured retinal images does not help to distinguish between possible optical etiologies for monocular diplopia. Rather, since the phenomenon clearly exists, the two possibilities are that the double-pass technique does not sufficiently resolve details of the line spread to find the effect, or there is no physical basis for monocular diplopia and it is entirely due to retinal processing effects.

LIMITATIONS ON PRODUCING A BIMODAL LINE SPREAD FUNCTION

As mentioned earlier, the hypothetical edge spread function shown in Figure 6 due to the line spread function shown in Figure 9, while useful for illustration purposes, is not physically possible. This can be seen by examining the corresponding point spread function from which this line spread function would have arisen. The point spread function can be recreated by taking the Fourier transform of the line spread function and the inverse Hankel transform of the resulting modulation transfer function (Figure 17). The problem is obvious from inspection of Figure 17: In order to produce a line spread function with a trough as deep as that seen in Figure 9, the central intensities of the point spread function would have to be negative.

As we have seen in the case of defocus alone, it is possible for the center of the defocused point spread function to drop to zero (Figure 11). But this is not the case for the line spread function. Figure 18 shows a barely physically possible point spread function obtained by truncating the negative intensity values of the point spread function shown in Figure 17 at zero. Integration along the chord through the center of the point spread function that gives rise to the center of the line spread function crosses the ring structure twice and will include only slightly less energy than a more peripheral chord that crosses the ring structure obliquely (Figure 19). So while all of the energy is in the ring structure and the intensity at the center of the point spread function is zero, this results in only a modest (18% contrast) trough in the center of the corresponding line spread function (Figure 20).

This more realistic hypothetical line spread function results in the edge spread function in Figure 21, and the gap in Figure 22, which is summarized for all possible gap widths in Figure 23, and results in an intensity ridge with only 5% contrast. While the limit is a contrast of 1 as the thickness of the peripheral ring approaches zero, the contrast illustrated in Figure 22 is probably close to the upper limit of what is physically realizable. This limit applies to any point spread function, whether it is due to diffraction alone or any aberration with radial symmetry (spherical aberration). The only way to obtain a trough in the line spread function with higher contrast (at least for some orientations) is with an asymmetric aberration that produces decreased intensity in various zones around the circumference of the ring structure of the point spread function.

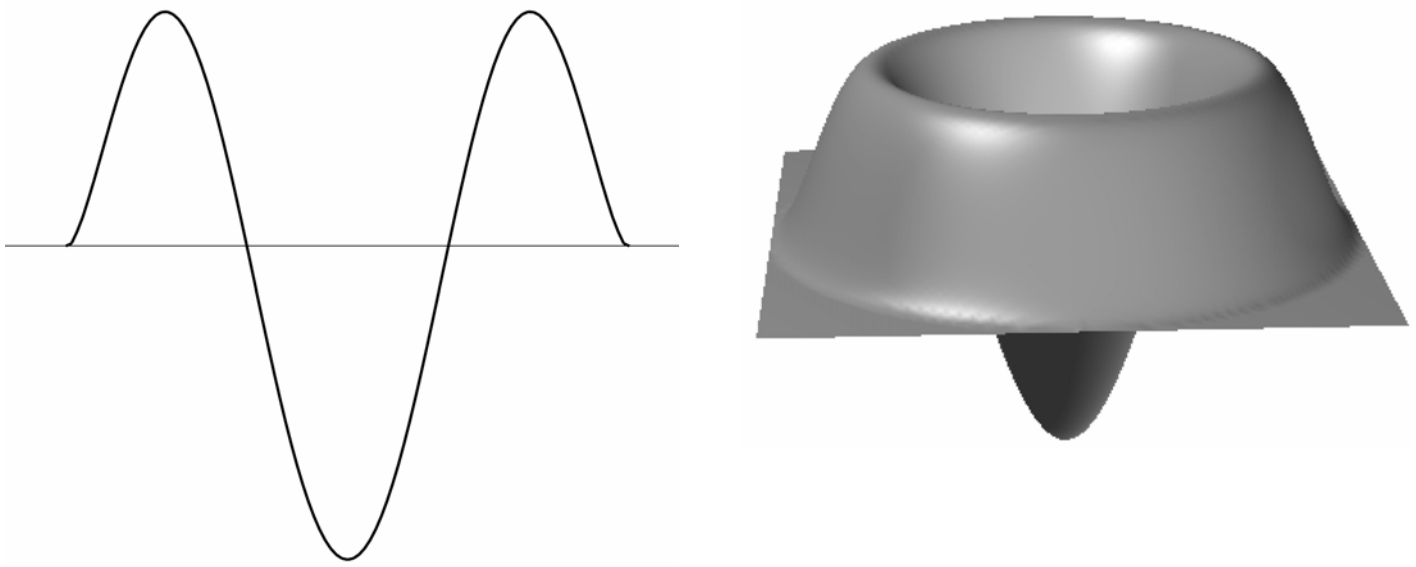

FIGURE 17

The impossible point spread function that would be needed to produce the hypothetical line spread function in Figure 9. Negative intensities, which cannot be physically realized, are necessary in the central area of the point spread function to create the deep trough in the center of the line spread function in Figure 9 and consequent broad inflection in the edge spread function of Figure 6. Left, Cross-section. Right, Surface plot.

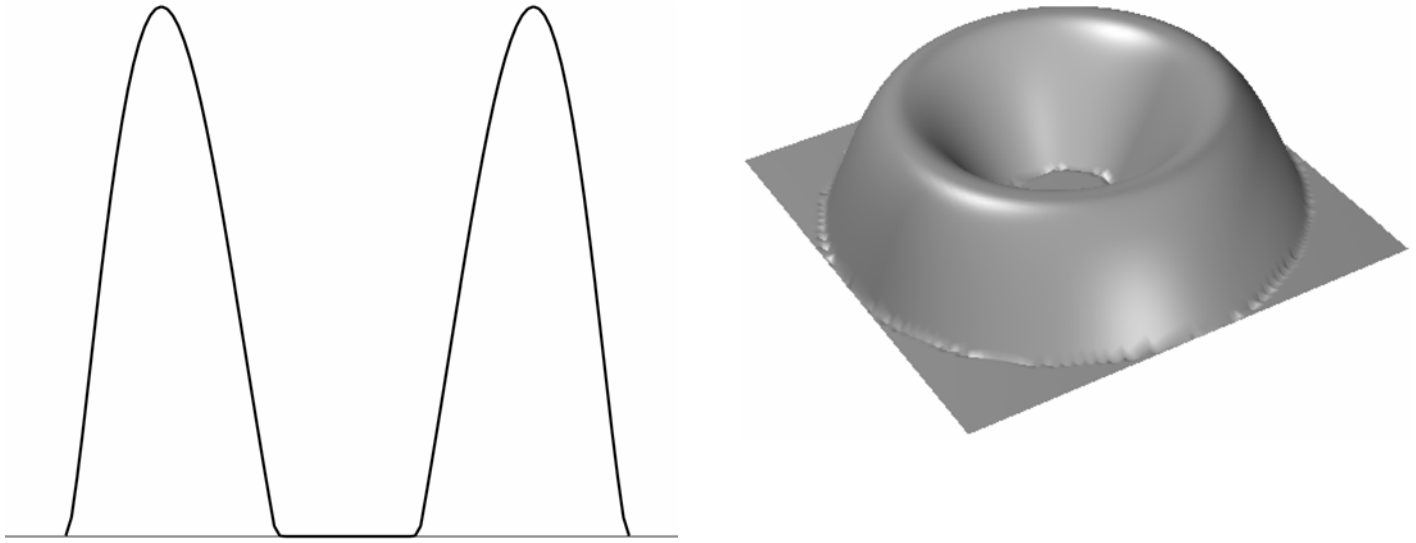

FIGURE 18

A point spread function as close as possible to that shown in Figure 17, yet physically realizable, can be created by truncating the negative central intensities to zero. Left, Cross-section. Right, Surface plot.

PUPIL SIZE

Considerations related to pupil size, both large and small, have been cited as evidence against the importance of diffraction in the genesis of monocular diplopia. Coffeen and Guyton[37] stated that because monocular diplopia is eliminated by a pinhole, it cannot be a diffraction effect. Conversely, Woods and coworkers[59] regarded the effects of diffraction as minimal with a 6-mm pupil. However, while geometrical optics gives a better approximation in some circumstances than others, image formation is in fact always subject to diffraction effects, regardless of pupil size.

The modulation transfer function and diffraction image will be of the same form at any pupil size if the amount of defocus is equivalent, where the amount of defocus is defined as the distance between an aberration-free wavefront and the defocused wavefront at the edge of the pupil.[43] With a small pupil, it will take much more dioptric power to cause the wavefront to develop a comparable amount of deviation from an aberration-free wavefront at the edge of the pupil than with a larger pupil. So a pinhole can eliminate monocular diplopia by rendering the magnitude of the aberration (defocus or other) effectively negligible; however, it does not increase diffraction effects—it only increases their spatial scale, when there are comparable amounts of defocus.

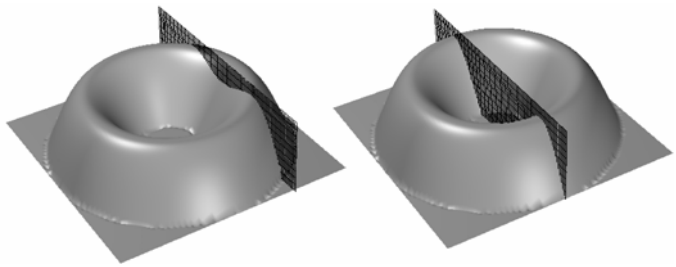

FIGURE 19

Integration along chords through the hypothetical point spread function in Figure 18 gives the corresponding line spread function. While the intensity falls to zero in the center of the point spread function, the central chord passes through the ring structure twice, yielding a fairly high intensity in the center of the line spread function and limiting the depth of the central trough.

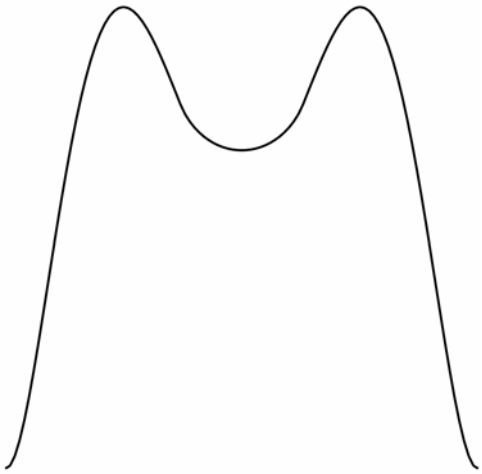

FIGURE 20

The line spread function calculated from the point spread function in Figure 18. There is a bimodal intensity distribution, but depth of the trough between the two peaks is limited.

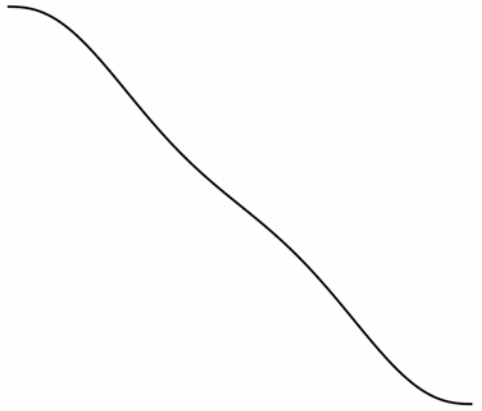

FIGURE 21

The physically realizable edge spread function calculated from the point spread function in Figure 20 has a much less prominent inflection than the hypothetical edge spread function in Figure 6.

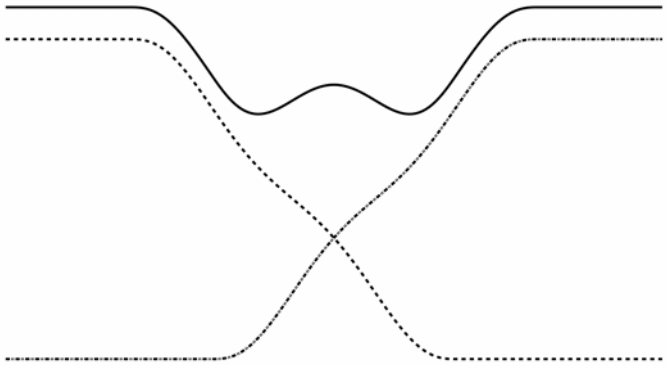

FIGURE 22

A black line constructed from two edges from Figure 21 (dashed lines). The summation of the two edges (solid line) has been shifted upward for clearer visualization. The intensity ridge that forms in gap is much smaller than in Figure 7. This is probably close to maximum contrast in the doubling of a black line that can be realized from any radially symmetric point spread function.

In diffraction theory, the main effect of pupil size is to determine the scale of the modulation transfer function and of the

diffraction image. With increasing pupil size, the scale of the modulation transfer function will increase proportionally and the scale of the diffraction image will decrease in inverse proportion. So relative to a 3-mm pupil, with the same amount of defocused wavefront deviation from an aberration-free wavefront at the pupil margin, the modulation transfer function with a 6-mm pupil will have the same shape but will be spread out over twice the range of spatial frequencies. On the other hand, the point spread function with a 6-mm pupil will be of the same shape, but will extend over only half of the angular subtense as that with a 3-mm pupil.

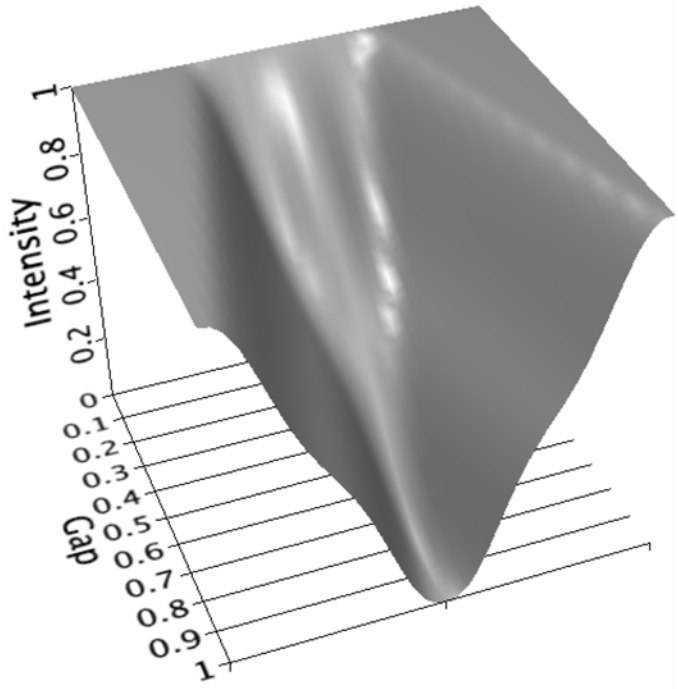

FIGURE 23

The intensity profile of a black line formed from two of the edges in Figure 21 as a function of the gap between the two edges of which it is comprised. The gap distance is plotted as a fraction of the edge spread width. As in Figure 8, a ridge forms in the gap to give the perception of splitting of the black line when the separation between the edges is less than half the width of the edge spread function; however, there is no gap width at which the contrast is any better than what is illustrated in Figure 22.

For an aberration-free system, it is mainly the diameter of the central bright spike in the diffraction pattern (Airy's disc) that is of interest in understanding resolving ability, with the very dim surrounding ring structure being of little consequence. With small pupil diameters, Airy's disc is large enough to be the limiting factor in resolving 2 points and the eye is said to be diffraction limited. For larger pupil diameters, the diameter of Airy's disc is small enough that it contributes negligibly to the broadening of the point spread function compared to the higher-order aberrations and scatter of the eye.[46] But that is not to say that the diffraction pattern is inconsequential in an eye with a large pupil when there is an error of focus. As the eye is defocused, energy is displaced from the central Airy's disc out into the ring structure of the diffraction pattern (yet the diameter of the central bright disc remains essentially unchanged, even with marked defocus, as seen in Figure 11; bottom right, this may explain why patients with uncorrected high myopia or aphakia are still able to localize targets reasonably accurately and retain surprisingly functional visual behavior). With defocus, the ring structure becomes the dominant feature of the point spread and, although more compressed with a larger pupil, will generally be of such dimensions that it is unlikely to be obscured by scatter and other aberrations.

HIGHER-ORDER ABERRATIONS

The effect of higher-order aberrations on image formation in an in-focus eye has been studied extensively; their impact for an eye with a defect of focus is less clear. Early work suggested the importance of spherical aberration[68,69]; on the other hand, Bour found that at higher spatial frequencies, at all pupil sizes, performance of the eye was determined by irregular and asymmetric monochromatic aberrations.[61] Howland and Howland found that monochromatic aberrations of the eye are of lesser importance.[70] Others have noted that among monochromatic aberrations, irregular,[60] coma-like or other asymmetric aberrations dominate.[71,72] Still, the population mean, aside from a small amount of positive spherical aberration, is zero for higher-order aberrations,[73] drawing into question whether these aberrations could be responsible for a general phenomenon. Additionally, the effect from the average amount of higher-order

aberrations for a 7.5-mm pupil is small relative to a defect of focus, amounting to less than the amount of wavefront error from 0.25 D defocus.[74]

Spherical Aberration

Arguing from a geometrical optics model, a number of investigators[30,35,37,40] have attributed the monocular diplopia occurring with ordinary refractive errors to the additional influence of spherical aberration. Using a geometrical optics model that incorporated the transverse aberration measured for each test subject, Woods and coworkers[41] predicted bimodal line spread functions with hyperopic (but not myopic) defocus that corresponded well with the subjects' actual observations of monocular diplopia. They concluded that the combination of hyperopia and the positive spherical aberration found in these subjects explained the monocular diplopia; however, without comparison calculations based on defocus alone, the importance of including spherical aberration in the prediction of the line spread function is unclear. Of course, a diffraction model would be needed for this comparison, since a bimodal line spread function could never arise from defocus alone in a geometrical optics model. Atchison and colleagues[75] did use a diffraction model in a subsequent study to calculate the effect of defocus on the contrast sensitivity function, but line spread function predictions without inclusion of the subjects' measured aberrations were not studied.

There are a number of reports that examine the theoretical effects of spherical aberration on image formation and modulation transfer functions using a diffraction model.[76-79] Because of the number of interdependent parameters with defocus, third-order, and fifth-order spherical aberration, it is difficult to make any general prediction as to whether including spherical aberration in an optical model will be constructive for development of monocular diplopia. Under most combinations of spherical aberration and defocus, the modulation transfer function develops undulations (zero crossings, in particular; see "Notches in the Contrast Sensitivity Function" section below) that may be related to monocular diplopia; however, it is unclear whether they exceed those produced by defocus alone.[77,78]

Inspection of ray diagrams of spherical aberration suggests that it should prevent the central intensity of the point spread function from dropping to zero, as occurs with various amounts of defocus alone, which could inhibit the development of monocular diplopia. This seems to be borne out experimentally by images at various points in the caustic curve, although it does appear that spherical aberration enhances the redistribution of energy from the central diffraction pattern to the more peripheral ring structure for image planes on the marginal side of the caustic curve,[56] which would support the development of monocular diplopia. In his analysis however, Barakat[76] found that light displaced from the central part of the diffraction image by spherical aberration did not go into forming higher maxima in the peripheral ring structure, but rather was scattered into the field more or less uniformly.

The occurrence of monocular diplopia with both positive and negative defocus presents a major problem for invoking spherical aberration as the explanation. Negative spherical aberration should produce diplopia only with myopic defocus[30,35] and positive spherical aberration only with hyperopic defocus.[30,41] Indeed, observing different effects on each side of best focus can be used as a sensitive test for the presence of spherical aberration[56]; however, the images of the point spread obtained by Villegas and colleagues[66] were reasonably symmetric for eyes with positive and negative defocus up to 2 D. Although monocular diplopia is reported only with hyperopic defocus by some[41,44] and only with myopic defocus by others,[35] Coffeen and Guyton[37] consistently demonstrated monocular diplopia with both hyperopic and myopic defocus in most individuals. To explain diplopia with both hyperopic and myopic defocus, they propose that the aberration increases out to a certain distance from the center of the pupil, after which it decreases. However, measurement of actual aberrations indicates that there is considerable variation from one person to another[57,68,72,80,81] and that the pattern of aberration proposed by Coffeen and Guyton would be unusual (as is negative spherical aberration in general, except perhaps in children).[41,68,80] Thus, it is unlikely that this specific and unusual pattern of aberration occurs consistently enough to explain the prevalence of monocular diplopia.

Coma

For reasons discussed above, asymmetric aberrations have more potential for producing line spread functions consistent with monocular diplopia than aberrations with radial symmetry. Coma has been implicated as an independent cause of monocular diplopia.[82] Coma after laser in situ keratomileusis is reported to be associated with monocular diplopia, whereas spherical aberration is associated more with symptoms of starburst and glare.[83]

Campbell and coworkers[57] found that coma usually occurs in association with spherical aberration but may be present independently in some eyes as well. A substantially non-zero phase transfer function in many eyes also provides evidence of asymmetric aberrations.[84-86] On the other hand, the aerial images of the point spread in emmetropic human eyes found by Santamaría and coworkers[87] were reasonably symmetric. When Artal and coworkers[88] calculated aberration functions from these point spreads, they found relatively little coma-like aberration with astigmatism being the most important asymmetric regular aberration. Whereas some investigators report a prevalence of coma-like asymmetric aberrations that may enough to explain the common occurrence of monocular diplopia with defocus,[60,71,72] coma could only account for diplopia of lines in one orientation and may be a more suitable explanation for the physiological (vertical) monocular diplopia described by Fincham.[32]

Notches in the Contrast Sensitivity Function

Apkarian and coworkers[36] noted notches in the contrast sensitivity function of subjects in whom they induced monocular diplopia by simulating small amounts of astigmatism. The spatial frequency of the notch was found to be $(2d)^{-1}$, where d is the separation of the diplopic images. This relationship suggests that the notch and the diplopia are both manifestations of the same phenomenon. Woods and coworkers[59] developed this further when they were able to predict notches in the contrast sensitivity function from their

geometrical optics model that included the measured transverse aberration function of subjects in whom hyperopia was simulated. They propose that these notches (and the associated monocular diplopia) are due to an interaction between the defocus and spherical aberration. With diffraction theory, however, defocus alone can account for notches in the contrast sensitivity function (zero crossings in the modulation transfer function, Figure 10). Previous studies by Campbell and Green[62] and Charman[89] showed only subtle evidence of notches in the contrast sensitivity functions of defocused eyes, perhaps because their test stimulus was more polychromatic than that employed by Woods and coworkers. However, Campbell and Green's and Charman's subjects presumably had typical amounts of higher-order aberrations similar to the subjects tested by Woods and coworkers, so the presence or absence of notches in their data cannot be taken as evidence one way or another regarding the need to invoke spherical aberration to explain the notches.

While zero crossings in the modulation transfer function—implying notches in the contrast sensitivity function—and the development of a bimodal or multimodal line spread function both occur with defocus, it is unclear whether there is a causal relationship. In the theoretical diffraction model, for example, as defocus increases, zero crossings in the modulation transfer function actually develop before the earliest appearance of a central trough in either the line spread or point spread functions (Figure 10, top middle, 11, top middle, and 12, top middle). The geometrical optics model of defocus also provides an obvious counterexample. In this case, zero crossings occur with any defocus at all and shift to progressively lower spatial frequencies with increasing defocus[43,45]; yet a central trough in the line spread function is not predicted at any amount of defocus under a geometrical optics model (Figure 2).

SEGMENTATION OF CRYSTALLINE LENS

Bour and Apkarian[90] showed in a theoretical study that a circular segment of refractive discontinuity could produce notches in the contrast sensitivity function and associated monocular polyopia. This study used mean values from other aberrometry studies, but it is unclear whether individuals with aberrations matching their model are common. Others have noted islands of different refractive power in the pupillary aperture,[91] and because some change with accommodation,[92] they can be considered to be lenticular in origin. These aberration features are probably more consistent with physiologic monocular diplopia than monocular diplopia with defocus. Obstfeld[93] commented on 6 images of a candle flame; his –2.50 refractive error was uncorrected. He attributed this to a multiple pinhole effect from the Y-sutures of the lens. The radiating pattern of stars is also suspected of being related to the suture lines of the anterior lens.[94]

RETINAL EFFECTS

Border enhancement, the most classic example of which is the Mach band phenomenon, is thought to be due to neural processing of the retinal image.[95] It has been studied extensively by Remole[44] in the context of optical blur. The spatial extent of this border enhancement was found to be closely related to the extent of the blur. Its extent would thus be exactly that required to exaggerate a light band centered in a black line or a dark band centered in a white line. In his studies, Remole found monocular diplopia with hyperopic defocus that he was unable to attribute to border enhancement alone and surmised that the line spread function of which the adjacent edges of a black line are composed must have a bimodal intensity distribution. Given the limited depth of the trough in a line spread function that is possible, it is likely that some form of contrast enhancement is needed to reconcile the physically possible intensity distribution with the much stronger perceptual experience of monocular diplopia.

The Stiles-Crawford effect and its interaction with spherical aberration has been examined with respect to the modulation transfer function with defocus[58,96]; however, this has not been examined with regard to the distribution of energy in the point spread function itself, though the effect is generally regarded to be one of apodization. This would have the effect of reducing the energy in the ring structure of the point spread function and tend to moderate the conditions that can lead to monocular diplopia.

OPHTHALMIC OPTICAL INSTRUMENTS

Heier and Brinchmann-Hansen[97] used a diffraction model to examine the effect of minor focusing errors when photographs from a fundus camera are used to measure retinal vessel width. Line spread functions calculated for defocus yielded bimodal and multimodal intensity distributions similar to those presented in this thesis. They pointed out that the "various peaks" were "due to diffraction" but dismissed them as being "of minor importance." This is true when the imaged object is large relative to the dimensions of the point spread function; however, the monocular diplopia effect can be more important with fine lines. The standard lensometer provides a convenient example: if the ocular is defocused, doubling of the fine black lines in the reticule pattern is easily observed.

CLINICAL EVALUATION OF MONOCULAR DIPLOPIA

Monocular diplopia is almost always optical in origin. In any individual case, this is easily proven by elimination of the diplopia with the use of a pinhole.[30,98] Ordinary refractive errors should not be overlooked as a cause of monocular diplopia. Even with physician awareness, it is easy to overlook refractive errors in the presence of binocular diplopia, poor vision, or other causes of monocular distortion such as metamorphopsia of retinal origin.

Because subjective refraction can be unreliable when vision is poor, such as with amblyopia, and in some cases of astigmatism, objective refraction is mandatory for evaluation of monocular diplopia. Even in this age of ubiquitous autorefractors, retinoscopy is the preferred refraction technique because it forces the examiner to scrutinize the red reflex for unusual aberrations that cannot be recognized by an autorefractor.

SUMMARY

The basic features of a blurred retinal image that give rise to monocular diplopia that occurs with ordinary refractive errors can be predicted from diffraction theory. Higher-order aberrations—such as spherical aberration—are not a necessary condition but may, under some circumstances, enhance the features of monocular diplopia. The physical basis for monocular diplopia is relatively subtle, and enhancement by neural processing is probably needed to account for the robustness of the percept.

ACKNOWLEDGMENTS

Funding/Support: None.
Financial Disclosures: None.

REFERENCES

1. Emsley H. *Visual Optics*. Vol 1. 5th ed. London: Hatton Press; 1952:414-416.
2. von Helmholtz H. *Helmholtz's Treatise on Physiological Optics.* Southall JPC, ed. Trans from 3rd German ed. Vol 1. New York: Dover; 1962:188-192.
3. Morris RJ. Double vision as a presenting symptom in an ophthalmic casualty department. *Eye* 1991;5:124-129.
4. Lepore FE, Yarian DL. Monocular diplopia of retinal origin. *J Clin Neuroophthalmol* 1986;6:181-183.
5. Records RE. Monocular diplopia. *Surv Ophthalmol* 1980;24:303-306.
6. Bender MD. Polyopia and monocular diplopia of cerebral origin. *Arch Neurol Psychiatry* 1945;54:323-338.
7. Cass EE. Monocular diplopia occurring in cases of squint. *Br J Opthalmol* 1941;25:565-577.
8. Guyton DL. Diagnosis and treatment of monocular diplopia. In: *Focal Points 1984: Clinical Modules for Ophthalmologists.* San Francisco: American Academy of Ophthalmology; 1984:1-10.
9. Holt R. Monocular diplopia. *Br Orthopt J* 1953;10:82-83.
10. Morgan MW. A unique case of double monocular diplopia. *Am J Optom* 1955;32:70-87.
11. Cackett P, Weir C, Houston CA. Transient monocular diplopia resulting from the treatment of amblyopia. *J Pediatr Ophthalmol Strabismus* 2003;40:245-246.
12. Rubin ML. The woman who saw too much. *Surv Ophthalmol* 1972;16:382-383.
13. Landesman KP, Bornstein L. Monocular diplopia associated with retinal detachment surgery. *J Am Optom Assoc* 1985;56:926-927.
14. Stampfer KA, Tredici TJ. Monocular diplopia in flying personnel. *Am J Ophthalmol* 1975;80:759-763.
15. Nagy V, Módis L, Kertész K, Vámosi P, Balázs E, Berta A. Anterior polar cataract as a cause of monocular diplopia. *J Cataract Refract Surg* 2004;30:1596-1597.
16. Diamond S. Monocular diplopia. *Am J Ophthalmol* 1963;55:371-373.
17. Hirst LW, Miller NR, Johnson RT. Monocular polyopia. *Arch Neurol* 1983;40:756-757.
18. Rubin ML. The case of the dramatic impression. *Surv Ophthalmol* 1975;20:133-136.
19. Bowman KJ, Smith G, Carney LG. Corneal topography and monocular diplopia following near work. *Am J Optom Physiol Opt* 1978;55:818-823.
20. Carney LG, Liubinas J, Bowman KJ. The role of corneal distortion in the occurrence of monocular diplopia. *Acta Ophthalmol* 1981;59:271-274.
21. Ford JG, Davis RM, Reed JW, Weaver RG, Craven TE, Tyler ME. Bilateral monocular diplopia associated with lid position during near work. *Cornea* 1997;16:525-530.
22. Knoll HA. Bilateral monocular diplopia after near work. *Am J Optom* 1976;52:139-140.
23. Mandell RB. Bilateral monocular diplopia following near work. *Am J Optom* 1966;43:500-504.
24. Goss DA, Criswell MH. Bilateral monocular polyopia following television viewing. *Clin Eye Vision Care* 1992;4:28-32.
25. Hersh PS, Steinert RF, Brint SF. Photorefractive keratectomy versus laser in situ keratomileusis: comparison of optical side effects. Summit PRK-LASIK Study Group. *Ophthalmology* 2000;107:925-933.
26. Hersh PS, Shah SI, Durrie D. Moocular diplopia following excimer laser photorefractive keratectomy after radial keratotomy. *Ophthalmic Surg Lasers* 1996;27:315-317.
27. Mulhern MG, Foley NA, O'Keefe M, Condon PI. Topographical analysis of ablation centration after excimer laser photorefractive keratectomy and laser in situ keratomileusis for high myopia. *J Cataract Refract Surg* 1997;23:488-494.
28. Takei K, Sano Y, Achiron LR, et al. Monocular diplopia related to asymmetric corneal topography after laser in situ keratomileusis. *J Refract Surg* 2001;17:652-657.
29. Wyzinski P, O'Dell L. Subjective and objective findings after radial keratotomy. *Ophthalmology* 1989;96:1608-1611.
30. Amos JF. Diagnosis and management of monocular diplopia. *J Am Optom Assoc* 1986;53:101-115.
31. Milder MR, Rubin ML. *The Fine Art of Prescribing Glasses*. Gainesville, Florida: Triad; 1978:240.
32. Fincham EF. Monocular diplopia. *Br J Ophthalmol* 1963;47:705-712.
33. Hales RH. Monocular diplopia: its characteristics and response to guanethidine. *Am J Ophthalmol* 1967;63:459-465.
34. Bull GJ. The visual effects of refractive error. *Trans Ophthalmol Soc U K* 1896;16:200-247.
35. Scott AB. Diplopia in myopia. *Surv Ophthalmol* 1974;19:166-168.

36. Apkarian P, Tijssen R, Spekreijse H, Regan D. Origin of notches in CSF: optical or neural? *Invest Ophthalmol Vis Sci* 1987;28:607-612.
37. Coffeen P, Guyton DL. Monocular diplopia accompanying ordinary refractive errors. *Am J Ophthalmol* 1988;105:451-459.
38. Charman WN, Jennings JAM. The optimal quality of the monochromatic retinal image as a function of focus. *Br J Physiol Opt* 1976;31:119-134.
39. Lamberts RL, Higgins GC, Wolfe RN. Measurement and analysis of the distribution of energy in optical images. *J Opt Soc Am* 1958;48:487-490.
40. Verhoeff FH. The cause of a special form of monocular diplopia. *Arch Ophthalmol* 1900;29:565-572.
41. Woods RL, Bradley A, Atchison DA. Monocular diplopia caused by ocular aberrations and hyperopic defocus. *Vision Res* 1996;36:3597-3606.
42. Hecht E, Zajac A. *Optics*. Reading, Massachusetts: Addison-Wesley; 1974:100.
43. Hopkins HH. The frequency response of a defocused optical system. *Proc R Soc A* 1955;231:91-103.
44. Remole A. Relation between border enhancement extent and retinal image blur. *Vision Res* 1974;14:989-995.
45. Smith G. Ocular defocus, spurious resolution and contrast reversal. *Ophthalmic Physiol Opt* 1982;2:5-23.
46. Westheimer G. Pupil size and visual resolution. *Vision Res* 1964;4:39-45.
47. Gubish RW. Optical performance of the human eye. *J Opt Soc Am* 1967;57:407-415.
48. Hopkins HH. The application of frequency response techniques in optics. *Proc Phys Soc* 1962;79:889-919.
49. Linfoot EH. *Fourier Methods in Optical Image Evaluation*. 1st ed. London: Focal Press; 1964:21-22, 82.
50. Oppenheim AV, Schafer RW. *Digital Signal Processing*. Englewood Cliff, New Jersey: Prentice-Hall; 1975:26-30, 290-321.
51. Press WH, Flannery BP, Teukolsky SA, Vetterling WT. *Numerical Recipes in C*. Cambridge, MA: Cambridge University Press; 1988:182-189, 403-418, 467-470.
52. Steel WH. The defocused image of sinusoidal gratings. *Optica Acta* 1956;3:65-74.
53. De M. The influence of astigmatism on the response function of an optical system. *Proc R Soc A* 1955;233:91-104.
54. Lamberts RL. Relationship between the sine-wave response and the distribution of energy in the optical image of a line. *J Opt Soc Am* 1958;48:490-495.
55. Lindberg P. Measurement of contrast transmission characteristics in optical image formation. *Optica Acta* 1954;1:80-89.
56. Cagnet M, Françon M, Thrierr JC. *Atlas of Optical Phenomena*. Berlin: Springer-Verlag; 1962:21-27.
57. Campbell MCW, Harrison EM, Simonet P. Psychophysical measurement of the blur on the retina due to optical aberrations of the eye. *Vision Res* 1990;30:1587-1602.
58. van Meeteren A. Calculations on the optical modulation transfer function of the human eye for white light. *Optica Acta* 1974;21:395-412.
59. Woods RL, Bradley A, Atchison DA. Consequences of monocular diplopia for the contrast sensitivity function. *Vision Res* 1996;36:3587-3596.
60. Krauskopf J. Further measurements of human retinal images. *J Opt Soc Am* 1964;54:715-716.
61. Bour LJ. MTF of the defocused optical system of the human eye for incoherent monochromatic light. *J Opt Soc Am* 1980;70:321-328.
62. Campbell FW, Green DG. Optical and retinal factors affecting visual resolution. *J Physiol* 1965;181:576-593.
63. Wilson BJ, Decker KE, Roorda A. Monochromatic aberrations provide an odd-error cue to focus direction. *J Opt Soc Am A* 2002;19:833-839.
64. Artal P. Calculations of two-dimensional foveal retinal images in real eyes. *J Opt Soc Am A* 1990;7:1374-1381.
65. Losada MA, Navarro R. Point spread function of the human eye obtained by a dual double-pass method. *Pure Appl Opt* 1998;7:L7-L13.
66. Villegas EA, González C, Bourdoncle B, Bonnin T, Artal P. Correlation between optical and psychophysical parameters as a function of defocus. *Optom Vis Sci* 2002;79:60-67.
67. Westheimer G, Campbell FW. Light distribution in the image formed by the living human eye. *J Opt Soc Am* 1962;52:1040-1045.
68. Ivanoff A. About the spherical aberration of the eye. *J Opt Soc Am* 1956;46:901-903.
69. Koomen M, Tousey R, Scolnik R. The spherical aberration of the eye. *J Opt Soc Am* 1949;39:370-376.
70. Howland B, Howland HC. Subjective measurement of high-order aberrations of the eye. *Science* 1976;193:580-582.
71. Howland HC, Howland B. A subjective method for the measurement of monochromatic aberrations of the eye. *J Opt Soc Am* 1977;67:1508-1518.
72. Walsh G, Charman WN, Howland HC. Objective technique for the determination of monochromatic aberrations of the human eye. *J Opt Soc Am A* 1984;9:987-992.
73. Thibos LN, Bradley A, Hong X. A statistical model of the aberration structure of normal, well-corrected eyes. *Ophthalmic Physiol Opt* 2002;22:427-433.
74. Thibos LN, Hong X, Bradley A, Cheng X. Statistical variation of aberration structure and image quality in a normal population of healthy eyes. *J Opt Soc Am A* 2002;19:2329-2348.
75. Atchison DA, Woods RL, Bradley A. Predicting the effects of optical defocus on human contrast sensitivity. *J Opt Soc Am A* 1998;15:2536-2544.

76. Barakat R. Total illumination in a diffraction image containing spherical aberration. *J Opt Soc Am* 1961;51:152-157.
77. Black G, Linfoot EH. Spherical aberration and the information content of optical images. *Proc R Soc A* 1957;239:522-540.
78. Goodbody AM. The influence of spherical aberration on the response function of an optical system. *Proc Phys Soc* 1958;72:411-424.
79. Kapany NS, Burke JJ. Various image assessment parameters. *J Opt Soc Am* 1962;52:1351-1361.
80. Jenkins TCA. Aberrations of the eye and their effects on vision: part 1. *Br J Physiol Opt* 1963;20:59-91.
81. Walsh G, Charman WN. Measurement of the axial wavefront aberration of the human eye. *Ophthalmic Physiol Opt* 1985;5:23-31.
82. Melamud A, Chalita MR, Krueger RR, Lee MS. Comatic aberration as a cause of monocular diplopia. *J Cataract Refract Surg* 2006;32:529-532.
83. Chalita MR, Xu M, Krueger RR. Correlation of aberrations with visual symptoms using wavefront analysis in eyes after laser in situ keratomileusis. *J Refract Surg* 2003;19:S682-S686.
84. Artal P, Santamaría J, Bescós J. Phase-transfer function of the human eye and its influence on point-spread function and wave aberration. *J Opt Soc Am A* 1988;5:1791-1795.
85. Charman WN, Walsh G. The optical phase transfer function of the eye and the perception of spatial phase. *Vision Res* 1985;25:619-623.
86. Walsh G, Charman WN. The effect of defocus on the contrast and phase of the retinal image of a sinusoidal grating. *Ophthalmic Physiol Opt* 1989;9:389-404.
87. Santamaría J, Artal P, Bescós J. Determination of the point-spread function of human eyes using a hybrid optical-digital method. *J Opt Soc Am A* 1987;4:1109-1114.
88. Artal P, Santamaría J, Bescós J. Retrieval of wave aberration of human eyes from actual point-spread-function data. *J Opt Soc Am A* 1988;5:1201-1206.
89. Charman WN. Effect of refractive error in visual tests with sinusoidal gratings. *Br J Physiol Opt* 1979;33:10-20.
90. Bour L, Apkarian P. Segmented refraction of the crystalline lens as a prerequisite for the occurrence of monocular polyopia, increased depth of focus, and contrast sensitivity notches. *J Opt Soc Am A* 1994;11:2769-2776.
91. Smirnov MS. Measurement of wave aberration in the human eye. *Biophysics* 1961;6:52-65.
92. van den Brink G. Measurements of the geometrical aberrations of the eye. *Vision Res* 1962;2:233-244.
93. Obstfeld H. The multiple image phenomenon. *Optom Vis Sci* 1991;68:79.
94. Navarro R, Losada MA. Shape of stars and optical quality of the human eye. *J Opt Soc Am A* 1997;14:353-359.
95. Ratliff F, Hartline HK, Miller WH. Spatial and temporal aspects of retinal inhibitory interaction. *J Opt Soc Am* 1963;53:110-120.
96. Zhang X, Ye M, Bradley A, Thibos L. Apodization by the Stiles-Crawford effect moderates the visual impact of retinal image defocus. *J Opt Soc Am A* 1999;16:812-820.
97. Heier H, Brinchmann-Hansen O. Reliable measurements from fundus photographs in the presence of focusing errors. *Invest Ophthalmol Vis Sci* 1989;30:674-677.
98. Smith JL. Monocular diplopia. *J Clin Neuroophthalmol* 1986;6:184-185.